Hindawi
Advances in Civil Engineering
Volume 2020, Article ID 6564193, 11 pages
https://doi.org/10.1155/2020/6564193

Research Article

Liquefiable Ground Treatment Using Cruciform Section Probe Resonant Compaction Method: A Case Study in the Xitong Expressway, Eastern China

Guangyin Du,[1] Han Xia,[1] Jun Cai,[1] Huangsong Pan,[1] and Changshen Sun[2]

[1]*School of Transportation, Southeast University, Nanjing, Jiangsu 211189, China*
[2]*Zhejiang Provincial Institute of Communication Planning, Design and Research, Hangzhou, Zhejiang 310013, China*

Correspondence should be addressed to Han Xia; evansha@126.com

Received 18 July 2019; Accepted 6 January 2020; Published 30 January 2020

Academic Editor: Salvatore Grasso

The foundation treatment of liquefiable soil has always been an important part of construction. Sand liquefaction decreases the foundation capacity and can cause severe building, highway, or bridge engineering accidents. This study used self-developed cruciform section probe resonant compaction equipment (CSPRCE) to evaluate the applicability and reinforcement effect of the Xitong Expressway foundation. The cone penetration test (CPT) results showed that this soil was liquefiable ground requiring treatment before construction. Laboratory tests illustrated that the clay particle content was nearly 10% in the surface layer, indicating that the traditional resonant compaction probe (RCP) would not provide effective reinforcement; therefore, we adopted the new resonant compaction method (RCM) for the reinforcement process. The CPT and standard penetration test (SPT) results after foundation reinforcement indicated that the cruciform section probe resonant compaction method (CSPRCM) is suitable for treating the Xitong Expressway liquefiable foundation. Before reinforcement, 7-8 liquefiable soil layers were observed, whereas after reinforcement, no foundation testing points were liquefiable. Cone resistance and unit sleeve friction resistance were both improved by a factor of nearly 3 after the CSPRCM reinforcement. The CSPRCM has wider applicability than traditional vibrating compaction methods, especially for sites with a high content of silt and clay particles. The strengthening mechanism of the CSPRCM is a vibration hammer that generates vibrational energy to obliterate the original soil structure and render the sand completely liquefied; the soil particles then rearrange to form a new structure.

1. Introduction

For human beings, earthquakes represent one of the most severe natural disasters [1–6]. Ground liquefaction, which is frequently caused by earthquakes, is one of the most common engineering disasters, and it weakens the foundation bearing capacity, thus leading to uneven foundation settlement. Furthermore, such liquefaction results in dehiscence and inclination of the structure in addition to subgradation and embankment slippage. Past earthquakes have caused many casualties and property losses [7]. Chen et al. [8] reviewed recent large earthquakes and found that large areas of liquefaction occurred at these earthquake sites. Liquefaction risk has been evaluated by the results of SPT tests, based on the Emilia Romagna Earthquake [9, 10].

The idea of strengthening the cohesion-less soil foundation with the cruciform section probe resonant compaction method arose in the late 1960s, although Mitchell [11] indicated that further research in this field is unnecessary. At the beginning of the 1970s, the United States Foster Company manufactured vibrating rod compacting machines based on vibratory pile driving equipment. Janes [12] reported that this equipment was successfully used to treated fine sand with a silt foundation. Anderson [13] illustrated this method in terms of the equipment, construction methods, and economic characteristics through an application example. Massarsch [14] introduced the concept of resonance dense design into vibratory pile driving equipment formed by the resonant compaction method. Subsequently, researchers worldwide developed different

resonant rods to reinforce sandy soil foundations, and China began studying this method in the late 1990s. And we developed new cruciform section probe resonant compaction equipment (CSPRCE) with a cruciform section probe (CSP) [15] in recent years. This equipment has been successfully used recently to treat sand and silty sand soil foundations in the laboratory and the field [16–19].

This study focuses on the treatment of the Yangtze River estuary alluvial area interactive marine and terrestrial silty sand and sand soil foundations through the cruciform section probe resonant compaction method (CSPRCM) to evaluate the suitability for sand foundation discrimination and the effect of liquefiable ground treatment.

2. Site Description and Testing Equipment

2.1. Testing Site. The Xitong Expressway located in South Jiangsu Province connects Wuxi to Nantong City. The area of interest was a new delta plain subregion of the piled plain of the Yangtze River Delta, which is associated with marine and continental alternative deposition. The characteristics of the engineering geology are different from that of other coastal sites, with alternating soft soil and fine sand sediment foundation.

Loose sand and silt 20 m beneath the ground surface is the major concern for liquefaction and therefore is considered in this example, and Quaternary Holocene sand and silt are widely distributed. The silty sand and silty soil are coloured grey, blue grey, and yellowish grey, and the density is slight and medium. The characteristics of the engineering geology are shown in Table 1. The seismic intensity is approximately 7, and the basic seismic acceleration value is 0.1 g.

2.2. CSP Equipment. The working performance of the vibration hammer depends mainly on the excitation frequency, the eccentric moment of the exciter, the exciting force, and the amplitude. The vibration hammer used in this research was a three-phase asynchronous vibration motor, and this tool was an electric rotary vibration exciter that combines a power source with a vibration source. The equipment parameters are provided in Table 2.

The CSP consists of two vertical intersecting steel plates. The four vibratory wing edges of this equipment have continuous convex semicircular teeth, and each vibratory wing has a small even hole, while the bottom of the vibratory wings has a spun tooth. This equipment is shown in Figure 1. In our study, the thickness of the steel plate was 3 cm, and the width of the steel plate was 60 cm. The diameter of the small hole was 10 cm, and the distance between the two small holes was 80 cm. The length of the CSP can be freely chosen according to the depth of the liquefaction site. The purpose of incorporating small holes and convex semicircular teeth is to reduce the extent of lateral vibration, which is conducive to the transmission of energy and the dissipation of pore water pressure caused by vibration compaction.

2.3. Cone Penetration Test (CPT) Equipment. The specifications of the CPT probe met the Code for Investigation of Geotechnical Engineering Standards [20]. The section area of the cylindrical cone was 10 cm^2 with a diameter of 43.7 mm, the cone bottom tip angle was 60°, the truncated area of the cone bottom was 15 cm^2, the length of the sidewall friction cylinder was 218.5 mm, and the surface area of the friction cylinder was 300 cm^2 (Figure 2). The cone resistance q_c and unit sleeve friction resistance f_s were obtained from CPT testing [21].

2.4. Standard Penetration Test (SPT) Equipment. The SPT also met the Code for Investigation of Geotechnical Engineering Standards [22]. SPT equipment uses GXY-1C exploration drilling rig, as can be seen in Figure 3, and the specific parameters are shown in Table 3. The quality of the hammer was 63.5 kg, and the drop distance was 76 cm. The freefalling weight method of automatic decoupling was adopted in the SPT to reduce the frictional resistance between the guide rod and the hammer. If the hammer reached 30 hits and the penetration depth did not reach 30 cm, then the actual penetration depth was recorded. The SPT hit number was calculated using the following equation [22]:

$$N = n \times \frac{30}{\Delta S}, \tag{1}$$

where N is the SPT hit number and ΔS is the penetration depth according to the hit number.

The actual SPT numbers can be corrected by the following equation [22]:

$$N' = \alpha \cdot N, \tag{2}$$

where $N'$is the corrected SPT hit number and α is the corrected parameter according to the length of the guide rod, as shown in Table 4.

The measuring points of the SPT and CPT are shown in Figure 4. Points #1–#7 were the SPT points, and points #8-#9 were the CPT points. CPT points #8 and #12 represented points before the foundation treatment, and the other CPT points represented points after the foundation treatment.

2.5. Foundation Treatment Design. To evaluate whether the CSPRCM is suitable for reinforcing foundations, the soil parameters (e.g., the soil saturation, relative density, ground water level, penetration resistance, soil particle gradation, and treatment of soil thickness) of the testing site should first be analysed. The reinforcement depth can be determined by in situ and laboratory tests of the liquefaction site, and then the length of the vibratory rod, power of the vibratory hammer, and power of the hoisting machines must be chosen. Parameters such as the resonance frequency, vibration point spacing, and point vibration duration are determined by the CPT results. In this study, the foundation was treated according to the design route, and the pile spacing was 1.8 m (and can range from 1.5 m to 2.1 m based on the CPT results) (Figure 5). The crane suspended the vibrating rod over the specified area, and the piling site was in the opposite direction. The vibration hammer was used to

Table 1: Physical parameters of the sample soil layers.

Layer	Soil	w (%)	e	ρ/g (cm^3)	W_L (%)	W_P (%)
1-1	Silty clay, silt	29.4	0.830	1.90	32.7	20.1
1-2c	Silty sand, silt	28.6	0.828	1.90	29.6	20.3
1–3	Silty sand	27.4	0.780	1.92	34.3	20.4
2-3	Silty fine sand	28.3	0.782	1.91	—	—

Table 2: Parameters of the vibration hammer.

Static eccentric moment (N·m)	Motor power (kW)	Vibration frequency (r/min)	Exciting force (kN)	Amplitude (mm)
270	90	1000	360	7.6

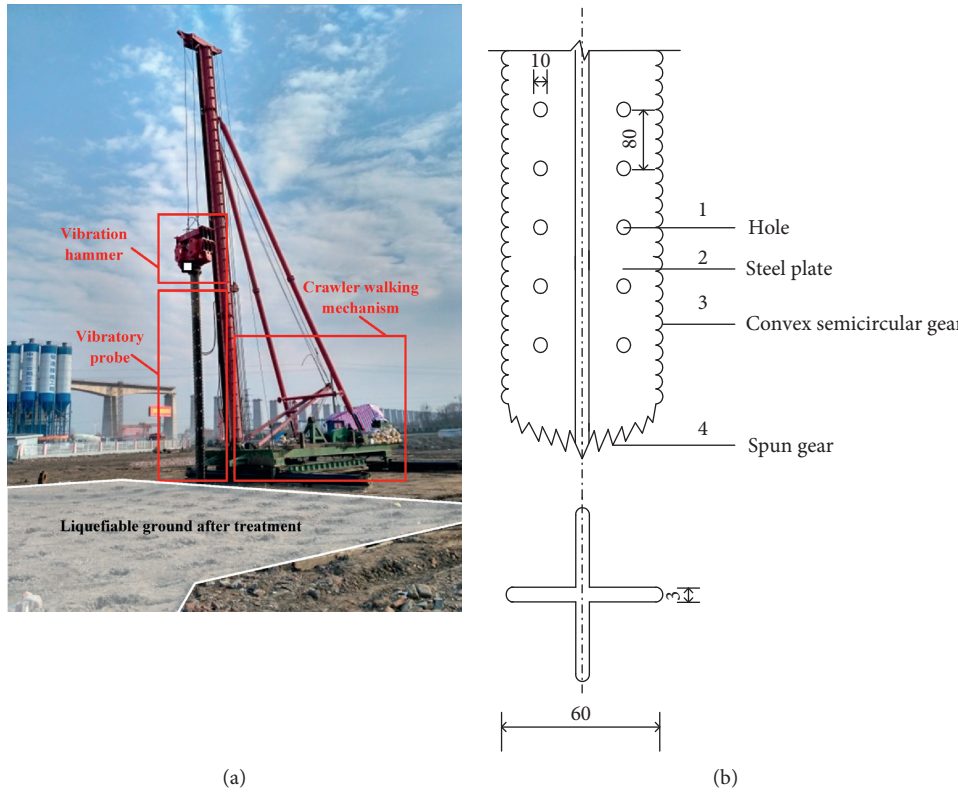

Figure 1: CSP resonant vibrating equipment. (a) CSPRCM equipment and (b) cruciform section vibrating probe (cm).

induce vibration in the vibratory rod until reaching the design depth. After the foundation treatment, the CPT, SPT, and lab tests were performed to evaluate the effect of reinforcement. The CSPRCM operation flow chart is shown in Figure 6.

3. Results and Discussion

3.1. Suitability for Densification. Two methods can be used to evaluate the treatment effect by the CSPRCM. First, the clay and silt particle contents are obtained through laboratory tests, and then the samples are indirectly evaluated by the cone resistance q_c and friction ratio R_f [23].

Before the foundation treatment, holes are drilled to sample the original soil, and a particle analysis experiment is used to test the content in each depth; the results are shown in Figure 7. For the top 2.5 m of this ground, the clay particle

Figure 2: CPT probe.

content reached 10%, and the silt particle content was above 49%, which can be classified as silt. The second soil layer clay content was more than 5%, and the silt particle content was above 35%; this type of soil can be defined as silty sand. At depths deeper than 5 m, clay and silt particle content decreased sharply, and the sand particle content exceeded 75%.

Mitchell [24] provided a method to evaluate whether the ground is suitable for use with the CSPRCM. The area of the

Figure 3: GXY-1C exploration drilling rig and SPT equipment.

Table 3: The parameters of GXY-1C exploration drilling rig.

Aperture (mm)	Hole depth (m)	Drill pipe diameter (mm)	Maximum pressure (kN)	Maximum pulling force (kN)
150/76/46	30/150/200	43	20	25

Table 4: Corrected rod parameters [22].

Rod length	≤3	6	9	12	15	18	21
A	1.0	0.92	0.86	0.81	0.77	0.73	0.70

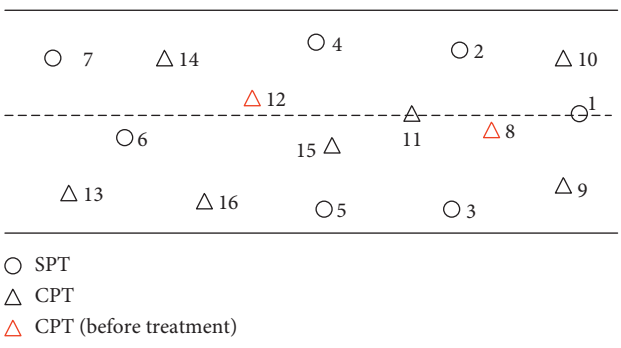

Figure 4: Layout of SPT and CPT measuring points.

two-dot line in Figure 6 was assigned (as Mitchell suggested) using the RCM to reinforce the foundation. A large part of the top 2.5 m of this ground was not suitable for use with the CSPRCM as a treated foundation. Half of the second soil layer grain size passed the curve beyond the Mitchell method area.

Figure 8 illustrates that the cone resistance and friction ratio are suitable parameters to evaluate soil densification with the Massarsch method [23]. The test points can be divided into the following three groups: easy to densify, capable of densifying, and difficult to densify. Clay and silt particles are difficult to compact with the traditional RCM, and sand particles are easily reinforced according to the traditional RCM method. The results of the two tests illustrated that the silt and clay particle contents significantly influenced the traditional RCM treatment effect. Therefore, the CSPRCM was suitable for evaluating the soils at this site, and the fine particle content was the key parameter for testing.

3.2. Primary Liquefiable Discrimination. Soil liquefaction is a common phenomenon of earthquake damage. Before construction, the possibility of building foundation liquefaction needs to be evaluated. Soil liquefaction preliminarily occurs in foundations according to one of the following three conditions [25]:

(1) In regions of 7 or 8 fortification intensity and a geological age after the Late Pleistocene of the Quaternary (Q_3);

(2) In regions of 7, 8, or 9 fortification intensity when the percentage of clay particles (particle size less than 0.005 mm) is less than 10, 13, or 16, respectively; and

(3) For buildings with a shallow natural foundation when the thickness of the overlying nonliquefied soils layer and the depth of the ground water level meet the following requirements [25]:

$$\begin{aligned} d_u &< d_0 + d_b - 2, \\ d_w &< d_0 + d_b - 3, \\ d_u + d_w &< 1.5d_0 + 2d_b - 4.5, \end{aligned} \tag{3}$$

where d_w is the depth of ground water (it is recommended to use the annual average water level from the past 10 years) (m), d_0 is the liquefied soil depth (m), d_b is the foundation depth (m), and d_u is the overlying nonliquefied soil layer thickness (it is recommended to subtract the depth of any organic mud soil layer) (m).

The clay particle results for seven percentage levels as determined by laboratory tests are shown in Table 5. The highest percentage of clay particles is 9.9% at depths of 2.0–2.3 m in the #3 test sample, and the percentage is still less than 10% of the standard recommended using SPT for the subsequent classification of liquefaction potential.

3.3. Classification of Liquefaction Potential before Reinforcement. The SPT procedure is adopted to evaluate the soil liquefaction potential by calculating the critical blow count. The critical blow count can be used in the following equation [22]:

$$N_{cr} = N_0\beta[\ln \mathrm{n}0.6d_s + 1.5n - 0.1d_w]\sqrt{\frac{3}{\rho_c}}, \tag{4}$$

where N_{cr} is the critical blow count in the SPT for classification, N_0 is the standard blow count in the SPT for classification (see Table 6), d_w is the ground water depth (m), ρ_c is the clay particle content percentage (if the clay particle

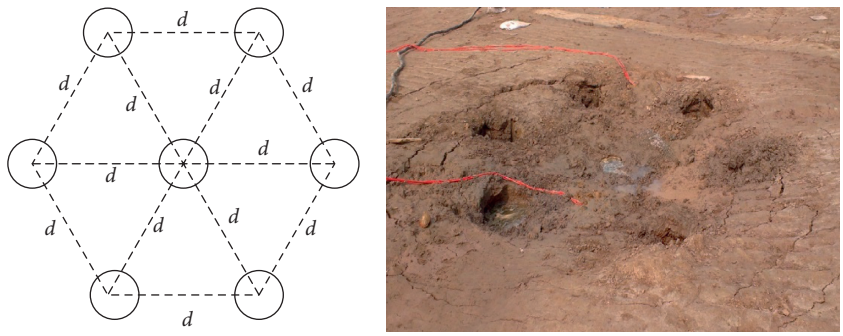

Figure 5: Layout of testing points in the resonance method ($d = 1.8$ m).

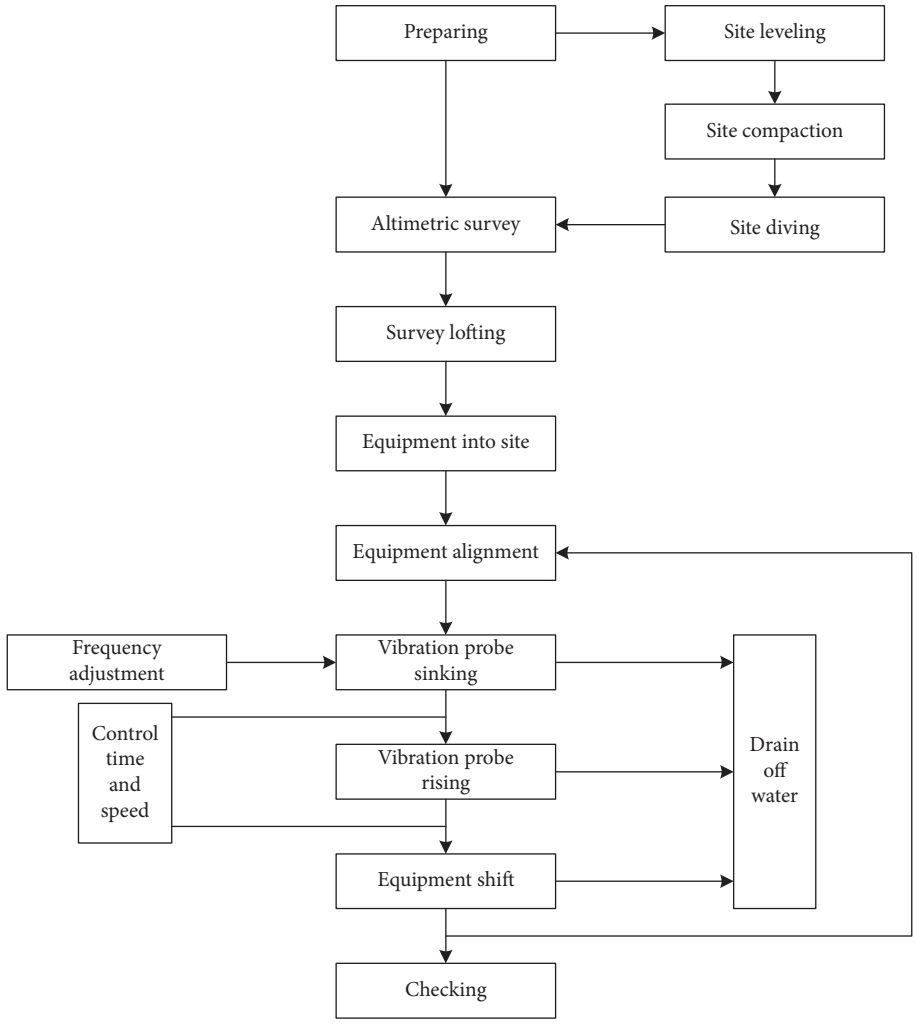

Figure 6: CSPRCM flow chart.

content percentage is less than 3%, use 3% instead of the actual value), and β is the adjustment coefficient (first group $\beta = 0.80$, second group $\beta = 0.95$, and third group $\beta = 1.05$). When the actual blow count in the SPT is more than the critical blow count, then this ground can be evaluated as a nonliquefiable field.

The CPT method is used to classify the liquefiable soil to calculate the critical cone tip resistance of liquefaction q_{ccr}. When the cone tip resistance is less than the value of the critical cone tip resistance, the soil should be classified as liquefiable soil and can be analysed using the following equation [22]:

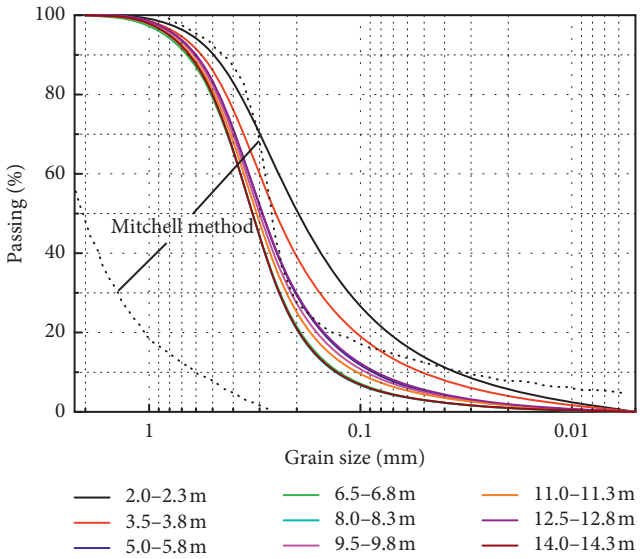

Figure 7: Particle size distribution for soils suitable for densification by CSPRCM.

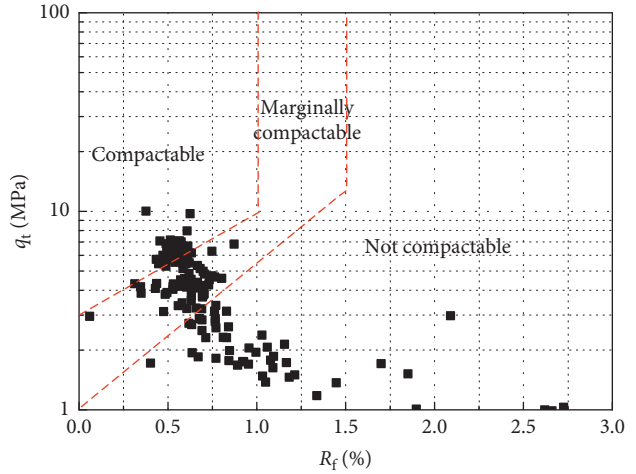

Figure 8: Compact ability evaluation based on the Massarsch method.

$$q_{ccr} = q_{c0}\alpha_w\alpha_u\alpha_p, \quad (5)$$

$$q_{ccr} = q_{c0}\alpha_w\alpha_u\alpha_p, \quad (6)$$

$$\alpha_w = 1 - 0.065(d_w - 2), \quad (7)$$

where q_{ccr} is the critical cone tip resistance, q_{c0} is the standard cone tip resistance (ground water depth is 2 m, overlying nonliquefiable soil layer is 2 m, see Table 7), α_w is the correction ground water parameter (the ground water has a hydraulic connection with underground water, $\alpha_w = 1.13$), α_u is the overlying nonliquefiable soil layer correction parameter (for a deep foundation, $\alpha_u = 1.0$), α_p is the correction parameter of the friction ratio (see Table 8), d_w is the ground water depth, and d_u is the overlying nonliquefiable soil layer thickness correction parameter.

Table 5: Percentage of clay particles in the Xitong expressway.

Depth (m)	Percentage of clay particle (%)						
	#1	#2	#3	#4	#5	#6	#7
2.0–2.3	9.3	7.8	9.9	8.4	8.9	9.8	9.5
3.5–3.8	6.5	9.1	7.2	5.9	7.8	8.6	9.6
5.0–5.3	2.3	2	2.5	0.6	1.9	2.7	2.1
6.5–6.8	1.2	1.4	0.4	0.9	1.2	1.1	2.3
8.0–8.3	1.4	0.3	1.4	1.2	1.5	2.1	0.8
9.5–9.8	2.5	2.1	1.8	0.4	2.1	2.2	1.5
11.0–11.3	2.4	2.3	1.5	2.9	2.3	0.9	0.7
12.5–12.8	2.8	3	2.9	2.4	2.9	2.4	2.4
14.0–14.3	1.4	2.1	1.4	0.8	1.2	1.6	1.6
15.5–15.8	—	—	—	0.8	1.2	1.6	0.7

Table 6: Standard blow count N_0 in SPT for classification of liquefaction potential [22].

Design earthquake acceleration (g)	0.10	0.15	0.20	0.30	0.40
Standard blow count in SPT/N_0	7	10	12	16	19

Table 7: Basic values of penetration resistance and cone tip resistance [22].

Seismic fortification intensity (MPa)	VII	VIII	IX
q_{c0}	4.6–5.5	10.5–11.8	16.4–18.2

Table 8: Soil correction coefficients [22].

Friction ratio/R_f (%)	Sand	Silt	
	$R_f \le 0.4$	$0.4 < R_f \le 0.9$	$R_f > 0.9$
α_p	1.0	0.60	0.45

The results of the classification of potential liquefaction with the CPT method are shown in Figure 8. As the depth increases, the cone tip resistance of the CPT holes #8 and #12 increase accordingly. To determine whether any soil layers are liquefiable soil, the critical cone tip resistance q_{ccr} should be calculated with equations (4)–(6). Based on the calculation results, the critical cone tip resistance q_{ccr} of the #8 hole can be divided into 8 parts, whereas that of the #12 hole can be divided into 7 parts. A comparison of the cone tip resistance qc and friction ratio R_f indicates that 6 layers can be evaluated as liquefiable soil (marked 1–6) in Figure 9(a) and that 5 layers can be evaluated as liquefiable soil (marked 1–5) in Figure 9(b). These results indicate that this area is liquefiable ground.

3.4. Liquefiable Discrimination after Reinforcement. As calculated using equation (4), the calculation results of the critical blow count in the SPT N_{cr} after the foundation treatment with the CSPRCM are shown in Table 9. As the depth increases, the critical blow count increases more sharply in the top 3 m on the ground and slowly later. Table 8 also includes the actual blow count in the SPT N and the ratio of N/N_{cr}. The actual blow count results in a remarkable increase at depths of 2–5 m and fluctuates at depths of

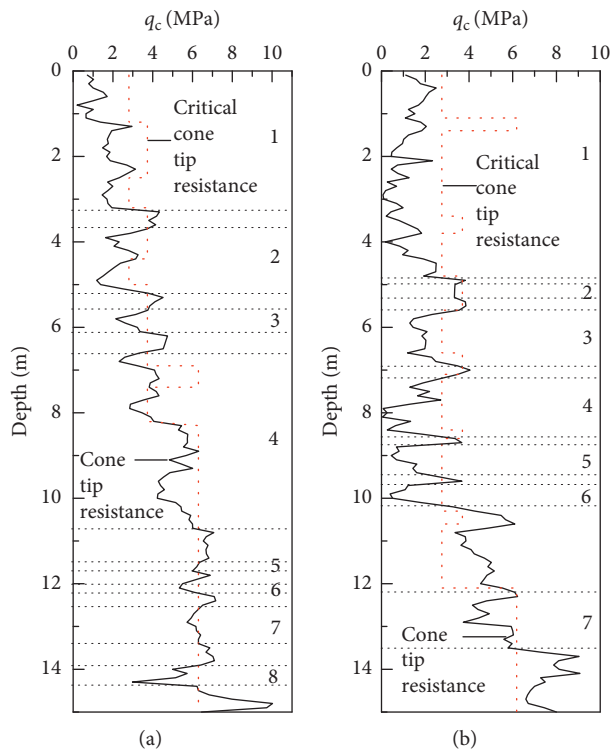

Figure 9: Soil liquefiable discrimination results before foundation treatment. (a) #8 CPT test result. (b) #12 CPT test result.

Table 9: Liquefiable evaluations by the SPT.

Hole number	Depth (m)	N	N_{cr}	N/N_{cr}
1	2.0–2.3	7	2.74	2.55
	3.5–3.8	7	6.43	1.09
	5.0–5.3	20	7.68	2.6
	6.5–6.8	30	8.70	3.45
	8.0–8.3	23	9.56	2.41
	9.5–9.8	28	10.31	2.72
	11.0–11.3	26	10.97	2.37
	12.5–12.8	25	11.56	2.16
	14.0–14.3	37	12.09	3.06
2	2.0–2.3	8	2.96	2.7
	3.5–3.8	9	3.67	2.45
	5.0–5.3	17	7.64	2.23
	6.5–6.8	27	8.66	3.12
	8.0–8.3	22	9.52	2.31
	9.5–9.8	26	10.27	2.53
	11.0–11.3	42	10.93	3.84
	12.5–12.8	39	11.52	3.39
	14.0–14.3	38	12.05	3.15
3	2.0–2.3	8	2.62	3.05
	3.5–3.8	11	6.38	1.72
	5.0–5.3	20	7.63	2.62
	6.5–6.8	20	8.65	2.31
	8.0–8.3	25	9.51	2.63
	9.5–9.8	28	10.26	2.73
	11.0–11.3	36	10.92	3.3
	12.5–12.8	40	11.51	3.48
	14.0–14.3	38	12.04	2.31
	—	—	—	—

Table 9: Continued.

Hole number	Depth (m)	N	N_{cr}	N/N_{cr}
4	2.0–2.3	13	2.85	4.56
	3.5–3.8	10	6.38	1.57
	5.0–5.3	14	7.63	1.83
	6.5–6.8	25	8.65	2.89
	8.0–8.3	25	9.51	2.63
	9.5–9.8	21	10.26	2.05
	11.0–11.3	28	10.92	2.56
	12.5–12.8	33	11.51	2.87
	14.0–14.3	30	12.04	2.49
	15.5–15.8	41	12.53	3.27
5	2.0–2.3	10	2.75	3.64
	3.5–3.8	10	6.36	1.57
	5.0–5.3	13	7.61	1.71
	6.5–6.8	19	8.63	2.2
	8.0–8.3	21	9.49	2.21
	9.5–9.8	25	10.24	2.44
	11.0–11.3	37	10.90	3.39
	12.5–12.8	41	11.49	3.57
	14.0–14.3	34	12.02	2.83
	15.5–15.8	35	12.51	2.8
6	2.0–2.3	8	2.62	3.05
	3.5–3.8	17	6.34	2.68
	5.0–5.3	18	7.59	2.37
	6.5–6.8	23	8.62	2.67
	8.0–8.3	29	9.48	3.06
	9.5–9.8	39	10.23	3.81
	11.0–11.3	30	10.89	2.75
	12.5–12.8	42	11.48	3.66
	14.0–14.3	36	12.01	3
	15.5–15.8	55	12.50	4.4
7	2.0–2.3	9	2.65	3.4
	3.5–3.8	13	3.54	3.67
	5.0–5.3	18	7.58	2.37
	6.5–6.8	24	8.60	2.79
	8.0–8.3	30	9.47	3.17
	9.5–9.8	35	10.21	3.43
	11.0–11.3	37	10.87	3.4
	12.5–12.8	30	11.46	2.62
	14.0–14.3	34	12.00	2.83
	15.5–15.8	34	12.49	2.75

5–15 m. From the laboratory tests for the particle size analysis in Figure 6, we conclude that the first 1-2 m is silty clay, an additional 1–4 m is silty sand, and the third soil layer is fine sand or sand. Therefore, the value of the actual blow count first increases and then fluctuates. The fluctuating value is not easily comparable to the critical blow count; thus, the value of N/N_{cr} is suitable for evaluation. A value of more than 1 indicates nonliquefiable soil, and a value less than 1 indicates liquefiable soil.

The results of the potential liquefaction evaluation by the CPT after foundation reinforcement by the CSPRCM are shown in Table 10. The critical cone tip resistance q_{ccr} of liquefaction was calculated by equation (5). As the depth increased, q_{ccr} and q_c increased. If the calculated value of q_{ccr} was less than the tested value of q_c, this soil was classified as a nonliquefiable foundation. To compare q_c and q_{ccr} more easily, the ratio q_c/q_{ccr} can be calculated. A ratio greater than 1 indicates nonliquefiable soil, and a ratio less than 1 indicates liquefiable soil. For values of q_c/q_{ccr} above 1, the soil after the CSPRCM treatment is nonliquefiable foundation, and the CPT evaluation result is the same as the SPT result.

Table 6 shows that the foundation reinforced by the CSPRCM is effective. Before the foundation treatment, 7-8 layers at a depth of 0–14 m are classified as liquefiable soil; and after foundation treatment, all of the 7 test points with different depths are classified as nonliquefiable soil.

3.5. Foundation Treatment Effect Evaluation on the CPT. The liquefaction foundation reinforcement effects through the CSPRCM can be reflected by the CPT results. Figure 10 shows the results of the foundation treatment effects of the CPT. The #8 and #12 holes are before treatment with the CSPRCM; the #9, #10, #11, #13, #12, and #16 holes are after

Table 10: Liquefiable evaluations by the CPT.

Hole number	Depth (m)	d_w (m)	q_c (MPa)	q_{ccr} (MPa)	q_c/q_{ccr}
9	0–1.5	1.34	3.52	2.83	1.24
	1.6–4.9	1.34	4.22	2.72	1.55
	5.0–9.6	1.34	7.77	2.30	3.38
	9.7–14.0	1.34	12.79	1.59	8.04
10	0–2.0	1.43	3.18	2.60	1.22
	2.1–4.4	1.43	4.12	2.89	1.43
	4.5–7.2	1.43	7.42	2.51	2.96
	7.3–14.0	1.43	11.20	1.76	6.36
11	0–2.7	1.40	4.02	3.02	1.33
	2.8–5.6	1.40	6.02	2.98	2.02
	5.7–9.5	1.40	8.95	2.24	3.40
	9.6–14.0	1.40	12.24	1.59	7.70
13	0–2.1	1.50	5.80	2.96	1.96
	2.2–6.1	1.50	5.63	2.64	2.13
	6.2–10.9	1.50	7.48	2.03	3.68
	11.0–15.0	1.50	12.95	1.34	9.66
14	0–2.8	1.46	3.33	2.75	1.21
	2.9–5.5	1.46	7.32	2.76	2.65
	5.6–10.6	1.46	9.18	2.14	4.29
	10.7–15.0	1.46	13.18	1.42	9.28
15	0–2.6	1.43	3.02	2.80	1.08
	2.7–7.6	1.43	6.91	2.87	2.41
	7.7–11.2	1.43	9.33	1.92	4.86
	11.3–15.0	1.43	13.72	1.38	9.94
16	0–3.0	1.50	3.0	2.42	1.24
	3.1–7.4	1.50	4.48	2.20	2.04
	7.5–9.7	1.50	8.71	2.05	4.25
	9.8–15.0	1.50	11.65	1.49	7.82

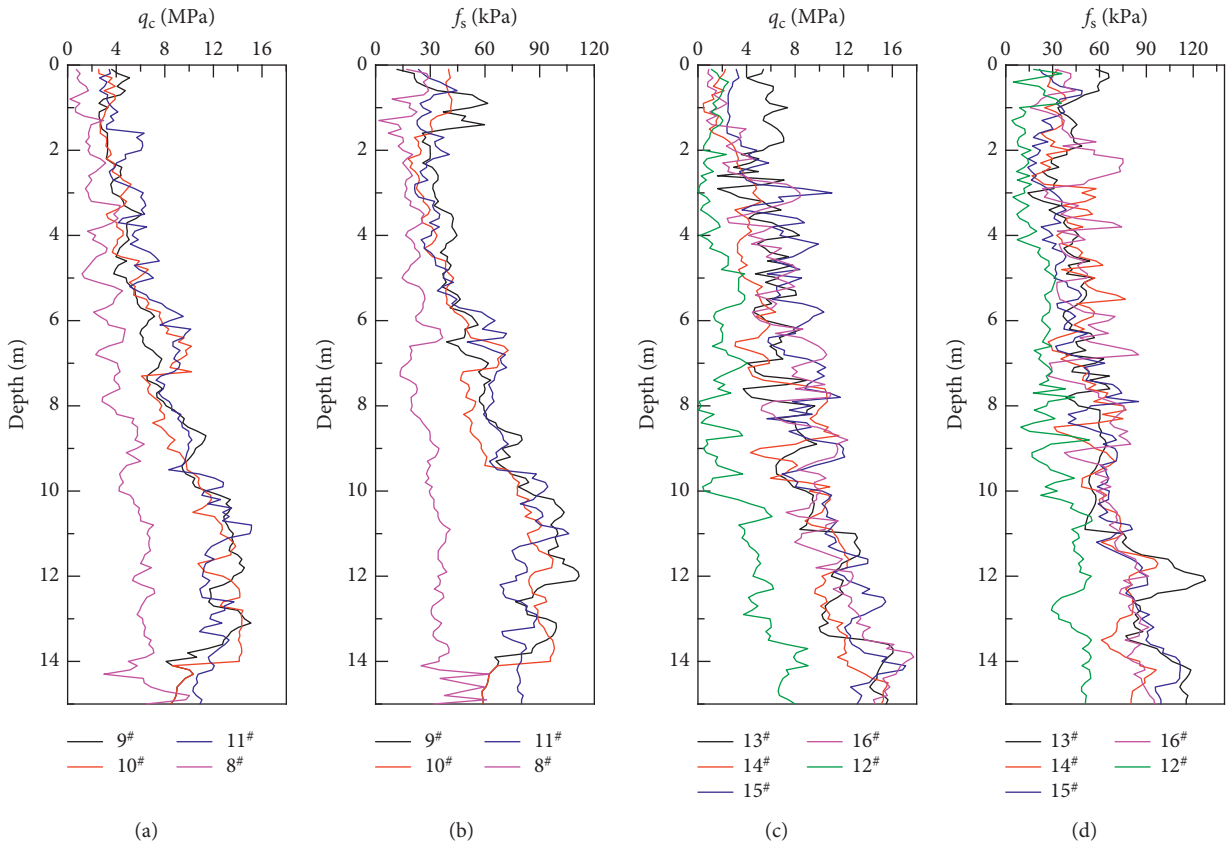

Figure 10: CPT results before and after foundation treatment with CSPRCM.

(a) (b)

Figure 11: Foundation reinforcement effect by CSPRCM. (a) Before and after reinforcement contrast. (b) Strengthening process.

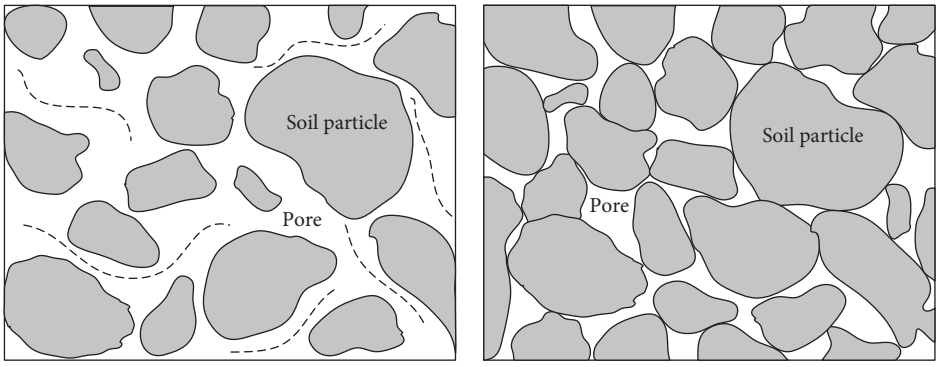

(a) (b)

Figure 12: Soil structure changes before and after reinforcement. (a) Before reinforcement. (b) After reinforcement.

reinforcement. Both the cone tip resistance q_c and side friction f_s increase with increasing depth. Before treatment, the cone tip resistance q_c fluctuates in the range of 0–9 MPa and the side friction f_s ranges from 0 to 45 kPa. After treatment, the cone tip resistance q_c and side friction f_s increase significantly. The largest value of q_c can reach 15 MPa, and the largest f_s can exceed 100 kPa. The resulting data indicate that foundation reinforcement with the CSPRCM can densify the soil.

3.6. Principle of CSPRCM Reinforcement. Figure 11 shows the strengthening effect of the foundation reinforcement by the CSPRCM. Figure 11(a) shows that the foundation before and after consolidation was greatly settled, which was mainly because the water in the soil was discharged during the reinforcement process (Figure 11(b)).

Applying the CSPRCM for sand layer reinforcement includes the incorporation of a strong vibration wave generated by the vibrating hammer that causes saturated sand liquefaction. Soil particles are suspended in water and move along with the pore water. After the pore water removes the soil, the soil particles gradually stagnate in the pores, and the density of the pores among the soil particles decreases. Then, the effective stress increases, and the soil gradually consolidates and becomes compressed and denser (see Figure 12).

4. Conclusions

This paper focuses on evaluating the reinforcement effect of the CSPRCM technique on liquefiable soils. A case study of the Xitong Expressway, eastern China, was carried out, and treatments for liquefiable soils were studied by SPT and CPT based methods. The results can be summarized as follows:

(1) The CSPRCM has suitable adaptability for treating the Xitong Expressway liquefiable foundation. According to the CPT test results, 7-8 liquefiable soil layers were observed before the resonance method was performed. The SPT and CPT results show that no foundation testing points were liquefiable after the CSPRCM reinforcement.

(2) Based on the CPT results, which characterized the foundation before and after the CSPRCM reinforcement, both the cone resistance and the unit sleeve friction resistance showed a nearly 3-fold improvement.

(3) The CSPRCM has wider applicability than the traditional vibrating compaction method. The effect of the traditional method is not suitable for high silt and clay content liquefiable foundations, although the CSPRCM can reinforce the sand foundation and improve the properties of the silt and silty sand.

(4) The strengthening mechanism of the CSPRCM involves a hammer that vibrates the soil to induce transverse and longitudinal waves. Through the vibration energy, the original structure of the soil is destroyed; the sand is completely liquefied; the pore water is discharged from the soil; and the pore sizes are reduced. Ultimately, the soil particles rearrange to form a new structure.

Data Availability

The figure and table data used to support the findings of this study are available from the corresponding author upon request. Email: evansha@126.com.

Conflicts of Interest

The authors declare that they have no conflicts of interest.

Acknowledgments

The authors gratefully acknowledge the financial support from the National Natural Science Foundation of China (grant no. 41372308). The authors also thank the Jiangsu Bureau of Transportation Engineering for their help with this study.

References

[1] E. M. Rathje, K. Kelson, S. A. Ashford et al., "Geotechnical aspects of the 2004 Niigata Ken Chuetsu, Japan, earthquake," *Earthquake Spectra*, vol. 22, no. 1_suppl, pp. 23–46, 2006.

[2] P. Monaco, F. Santucci de Magistris, S. Grasso, S. Marchetti, M. Maugeri, and G. Totani, "Analysis of the liquefaction phenomena in the village of Vittorito (L'Aquila)," *Bulletin of Earthquake Engineering*, vol. 9, no. 1, pp. 231–261, 2011.

[3] B. R. Cox, R. W. Boulanger, K. Tokimatsu et al., "Liquefaction at strong motion stations and in Urayasu city during the 2011 Tohoku-Oki earthquake," *Earthquake Spectra*, vol. 29, no. 1_suppl, pp. 55–80, 2013.

[4] J. Bray, M. Cubrinovski, J. Zupan, and M. Taylor, "Liquefaction effects on buildings in the central business district of christchurch," *Earthquake Spectra*, vol. 30, no. 1, pp. 85–109, 2014.

[5] J. Koseki, K. Wakamatsu, S. Sawada, and K. Matsushita, "Liquefaction-induced damage to houses and its countermeasures at Minami-Kurihashi in Kuki city during the 2011 Tohoku earthquake, Japan," *Soil Dynamics and Earthquake Engineering*, vol. 79, no. Part B, pp. 391–400, 2015.

[6] R. Verdugo and J. González, "Liquefaction-induced ground damages during the 2010 Chile earthquake," *Soil Dynamics and Earthquake Engineering*, vol. 79, no. Part B, pp. 280–295, 2015.

[7] Q. T. Yang, *The Shaking Table Experimental Study on Liquefiable Sand Soil Improve by Pile*, Taiyuan University of Technology, Taiyuan, China, 2008.

[8] G. X. Chen, X. F. Gu, X. D. Chang et al., "Review and implication of successful ground improvement cases about mitigating soil liquefaction induced by 8 strong earthquakes from 1989 to 2011," *Rock and Soil Mechanics*, vol. 4, no. 36, pp. 1102–1118, 2015.

[9] V. Fioravante, D. Giretti, G. Abate et al., "Earthquake geotechnical engineering aspects: the 2012 Emilia Romagna earthquake (Italy)," in *Proceedings of the 7th International Conference on Case Histories in Geotechnical Engineering*, Chicago, IL, USA, May 2013.

[10] A. Cavallaro, P. Capilleri, and S. Grasso, "Site characterization by dynamic in situ and laboratory tests for liquefaction potential evaluation during Emilia Romagna earthquake," *Geosciences*, vol. 8, no. 7, p. 242, 2018.

[11] J. K. Mitchell, "In-place treatment of foundation soils," *Journal of the Soil Mechanics and Foundations Division*, vol. 96, no. 1, pp. 73–110, 1970.

[12] H. W. Janes, "Densification of sand for drydock by Terra-Probe," *Journal of Soil Mechanics and Foundations Division*, vol. 99, no. 6, pp. 451–470, 1973.

[13] R. D. Anderson, "New method for deep sand vibratory compaction," *Journal of the Construction Division*, vol. 100, no. 1, pp. 79–95, 1974.

[14] K. R. Massarsch, "Deep soil compaction using vibratory probes," in *Deep Foundation Improvements: Design, Construction and Testing*, R. C. Bachus and M. I. Esrig, Eds., pp. 297–319, ASTM International, Baltimore, MD, USA, 1991.

[15] S. Y. Liu, G. Y. Du, and Y. H. Miao, Cruciform Section Probe, CN PET, 2007 10020591.9. 2008-12-24.

[16] G. Y. Du, S. Y. Liu, B. B. Ren, and L. Xie, "Application of treatment on liquefied foundation using resonance compaction method," *Journal of Engineering Geology*, vol. s1, no. 22, pp. 466–469, 2014.

[17] L. Xie, G. Y. Du, D. D. Miao, and Z. Y. Yang, "Effect evaluation of treatment on coastal liquefiable ground using resonant compaction method," *Journal of Engineering Geology*, vol. s1, no. 23, pp. 695–698, 2015.

[18] Y. Cheng, H. Zhu, F. Jing, G. Du, C. Yan, and Z. Liu, "Experimental research of spatial variation of compaction effect on vibratory probe compaction method for ground improvement," *Procedia Engineering*, vol. 189, pp. 466–471, 2017.

[19] Q. Guo, G. Du, C. Gao, T. Luo, and L. Xie, "Experimental study on influence of clay lens on compaction effect of resonant compaction method," *Journal Of Southeast University (Natural Science Edition)*, vol. 49, no. 3, pp. 427–432, 2019.

[20] GB 50021–2010, *Code for Investigation of Geotechnical Engineering*, Ministry of Housing and Urban-Rural Development of the People's Republic of China and Administration for Market Regulation, Beijing, China, 2009.

[21] W. Duan, S. Liu, and G. Cai, "Evaluation of engineering characteristics of lian-yan railway soft soil based on CPTU data-a case study," *Procedia Engineering*, vol. 189, pp. 33–39, 2017.

[22] DB32/T 2283-2012, *Inspection Specification for Cement Mixing Pile Quality of Highway Engineering*, Jiangsu Bureau of Quality and Technology Supervision, Nanjing, China, 2012.

[23] H. F. Zou, G. J. Cai, S. Y. Liu et al., "Evaluation of resonant method for improving liquefiable foundation based on CPTU soil behavior type index," *Chinese Journal of Rock Mechanics and Engineering*, vol. S2, no. 32, pp. 4106–4114, 2013.

[24] J. K. Mitchell, "Soil improvement: state-of-the-art report," in *Proceedings of the 10th International Conference on Soil Mechanics and Foundation Engineering*, pp. 509–565, Stockholm, Sweden, June 1981.

[25] GB 50011–2010, *Code for Seismic Design of Buildings*, Ministry of Housing and Urban-Rural Development of the People's Republic of China and Administration for Market Regulation, Beijing, China, 2010.